

Distribution Agreement

In presenting this thesis as a partial fulfillment of the requirements for a degree from Emory University, I hereby grant to Emory University and its agents the non-exclusive license to archive, make accessible, and display my thesis in whole or in part in all forms of media, now or hereafter now, including display on the World Wide Web. I understand that I may select some access restrictions as part of the online submission of this thesis. I retain all ownership rights to the copyright of the thesis. I also retain the right to use in future works (such as articles or books) all or part of this thesis.

Liam Horne

April 10, 2023

Effects of Phosphate Uptake/Metabolism on Behavior of Lung Cancer Cells

by

Liam Horne

George R. Beck Jr.
Adviser

Biology

George R. Beck Jr.
Adviser

Roger B. Deal
Committee Member

Dan Perrien
Committee Member

2023

Effects of Phosphate Uptake/Metabolism on Behavior of Lung Cancer Cells

By

Liam Horne

George R. Beck Jr.

Adviser

An abstract of

a thesis submitted to the Faculty of Emory College of Arts and Sciences

of Emory University in partial fulfillment

of the requirements of the degree of

Bachelor of Science with High Honors

Biology

2023

Abstract

Effects of Phosphate Uptake/Metabolism on Behavior of Lung Cancer Cells

By Liam Horne

Excess inorganic phosphate (Pi) availability has been suggested to have a role in cancer progression in preclinical mouse models. Cell-based studies have demonstrated that increased extracellular Pi alters proliferation, metabolism, and the migratory behavior of cells. Taken together, the results suggest that precancerous cells acquire a need for increased Pi consumption. An obstacle to assessing the Pi intake requirements of precancerous and cancerous cells is an inability to track cellular Pi consumption. In this study, a novel FRET-based fluorescent microscopy system was used with the A549 human lung adenocarcinoma cell line to track cytoplasmic Pi, as a measure of Pi consumption. The cells were sorted based on their FRET signal from the cytoplasm into subpopulations based on their Pi-consumption phenotype (high, moderate, and low PI-consuming). Assays to assess growth, migration, colony formation, and gene expression were performed to measure differences among the different Pi-consuming cell populations in normal and high Pi environments. Results showed that high Pi-consuming A549 cells demonstrated a phenotype with increased proliferation, and migration, along with upregulation of OPN, a secreted factor associated with cancer progression in various models. These findings show that high Pi-consumers have more of the characteristics associated with lung cancer progression, and thus Pi metabolism could offer a target for therapeutic intervention. The FRET sensor offers an intriguing look at how Pi consumption tracks with changes in cell behavior, particularly related to the early stages of cancer progression.

Effects of Phosphate Uptake/Metabolism on Behavior of Lung Cancer Cells

By

Liam Horne

George R. Beck Jr.

Adviser

A thesis submitted to the Faculty of Emory College of Arts and Sciences
of Emory University in partial fulfillment
of the requirements of the degree of
Bachelor of Science with High Honors

Biology

2023

Acknowledgments

I would like to acknowledge the Emory School of Medicine Beck Lab for the opportunity to use their facilities. Special thanks to Jamie Arnst and my committee members' help throughout the entire Honors process. My ability to do this would not have been possible without y'all's mentorship and guidance.

TABLE OF CONTENTS

INTRODUCTION.....	1
GOALS & HYPOTHESIS.....	2
METHODS/PROTOCOL	3
GENERATION OF FRET EXPRESSION CELL LINE	3
FACS SORTING.....	3
GROWTH TIME COURSE ASSAY.....	4
QUANTITATIVE REALTIME PCR (QRT-PCR).....	4
TABLE 1	5
MIGRATION/INVASION	5
COLONY FORMATION	5
STATISTICS	6
RESULTS	6
FIGURE 1. FLIPPI FRET BIOSENSOR	8
FIGURE 2. GROWTH AND PROLIFERATION RATES ARE DIFFERENT BETWEEN THE PI-CONSUMING SUB-POPULATIONS	9
FIGURE 3. HIGH PI CONSUMERS DO NOT FORM COLONIES AT GREATER RATES	11
FIGURE 4. HIGH PI CONSUMERS DEMONSTRATE AN INCREASED MIGRATORY PHENOTYPE.....	12
FIGURE 5. CHANGES IN GENE EXPRESSION	14
DISCUSSION	14
CONCLUSIONS/FUTURE DIRECTIONS.....	18
REFERENCES.....	19

Introduction

Lung cancer is one of the leading causes of death worldwide. Over 130,180 die every year from it in the United States. Insufficient treatment options exacerbate the health consequences further. The 2-year survival rate for individuals with non-small cell lung cancer (NSCLC) stands at less than 20%. [1] Ultimately, the metastasis of cancer cells is what is often deadly to the patient, and treatment for metastasis is limited causing survival rates to drop even more. [2] Cell motility and migration are important underlying events of the early stages of cancer metastasis. Understanding how tumor cells grow, proliferate, and migrate to other microenvironments in the body is extremely important to developing novel therapeutics thereby increasing patient survival. [3]

Inorganic Phosphate/phosphorus (Pi) plays a vital role in homeostatic processes across the body and in the maintenance of healthy cells. From ATP formation, and essential cell signaling pathways involving kinases, to the synthesis of biomolecules, Pi is an indispensable nutrient for cell growth. [4-8] Accordingly, tumors also have shown the ability to increase their uptake of Pi. [9-11] This makes sense, as tumors are rapidly growing, and need new Pi to synthesize DNA, RNA, and ribosomes, to make essential proteins. [9, 12] An increase in Pi uptake is found during cell mitosis, or during the division of cells, however, the physiological significance and/or dependence on Pi for tumor growth remains unclear. [13] Since tumor cells are defined by their increased rate of cellular division in comparison to normal tissues, targeting cellular Pi consumption to counteract cancer cell activity is a novel strategy for therapeutic intervention. In cell culture models, Pi strongly affects tumor cell proliferation and metabolism, and dietary Pi has been shown to increase lung cancer progression in a pre-clinical mouse model. [12, 14, 15] The idea that rapidly dividing cells require additional Pi is supported by one study

that found that tumor samples had 2x as much interstitial Pi as normal tissue samples in the tumor microenvironment. [9]

Cells regulate Pi uptake (consumption) by two families of Pi sodium-dependent co-transporters: Type-II (Slc34a1, Slc34a2, Slc34a3) and Type-III (Slc20a1, Slc20a2). [16, 17] The type-II family is mainly found in the kidney and gut and is mostly responsible for systemic Pi homeostasis. [18] Interestingly, Slc34a2 has been identified as overexpressed in lung cancer models. [19] Type-III transporters are more ubiquitously expressed and are thought to be involved in Pi homeostasis at the cell level. [20] Evidence exists of upregulation of these transporters in tumor cells, pointing towards Pi as an indicator of rapid cell tumorigenesis and subsequent tumor growth. [21] Because Pi is so common in cells one of the main challenges associated with studying the role of Pi in tumor cell growth and migration is the ability to track cell consumption and use.

Goals and Hypothesis:

The goal of this study is to define how Pi consumption affects lung cancer cell behavior, and how this affects lung cancer progression and metastasis. Also, this study seeks to find a method of reliably tracking Pi consumption by a novel fluorescent microscopy approach. The hypothesis to be tested is that high Pi-consuming lung cancer cells will have higher growth potential and more readily migrate, suggesting a precancerous phenotype.

To measure levels of Pi consumption, the sleeping beauty transposon system was used to introduce the FLIPPi Fluorescence Resonance Energy Transfer (FRET) system into the A549 line of human non-small cell lung cancer (NSCLC) cells. This FRET system produces a high FRET signal when free Pi levels in the cytoplasm are low. As free cytoplasmic Pi increases, the FRET signal decreases. Therefore, this system can track free cytoplasm Pi. Using Fluorescent

sorting subpopulations of cells were isolated based on high FRET (low Pi consumption), moderate FRET (medium Pi consumption), or low FRET (high Pi consumption). Cell subpopulations with a high Pi consumption phenotype demonstrated increased proliferation and an increased migratory phenotype. Further, inhibition of Pi-transport reduced cell migration and colony formation, suggesting the requirement of Pi consumption in both processes. Overall, this FRET system offers a promising starting point for tracking Pi consumption by NSCLC cells and illuminating mechanisms by which cell Pi consumption affects cell motility and metastasis.

Methods/Protocol:

Generation of FRET expressing cell lines:

The transposon vector containing the FLIPi cassette, and the transposase vector were transiently transfected using Lipofectamine (Invitrogen, Waltham, MA) into A549 cells in accordance with the manufacturer's protocol in a 5:1 ratio. [22] After 48h the media was changed and cells expressing FLIPi were selected for using puromycin at 2 μ g/ml (Sigma, St. Louis, MO). Cells were then FACS (Fluorescence-Activated Cell Sorting) sorted for YFP to eliminate any low or very high-expressing cells. This creates a large subpopulation that has a more homogenous expression without impacting the heterogeneity of the phenotype. All cells were grown in DMEM (Corning, Corning, NY) with 10% FBS (Atlanta, GA Biologics) and 1% Pen/Strep (HyClone, Logan, UT) at 37°C with 5%CO₂. Cells were regularly subcultured (every 2 to 3 days).

FACS sorting:

For the FACS sorting of the subpopulations, single cells were suspended in HBSS (HyClone) containing 1% FBS and 1mM EDTA (final Pi 0.7mM) for FACS-FRET sorting using a FACS Aria II (BD Bioscience, Franklin Lakes, NJ). To measure CFP, FRET cells were excited

with the 405 nm laser and fluorescence was measured with a standard 450/40 filter for CFP and a 529/24 filter for the FRET signal. To measure YFP, cells were excited with the 488 nm laser, and emission was collected with a 529/24 filter. Cellular populations were sorted based on high, low, or moderate FRET signals. Subpopulations were reevaluated for FRET signal, as described above, out to 20 passages to ensure phenotypic stability.

Growth Time Course Assay

The cell subpopulations analyzed were low FRET cells, moderate FRET cells, and high FRET cells. The three A549 FRET expressing cell lines were plated at 500 cells per well (96-well plate) in 100 μ l of DMEM with 10% FBS. XTT reagent (Promega, Madison, WI) was added (20 μ l) per the manufacturer's protocol. Plates were read on day 1, day 3, and day 5 at an absorbance of 490 nm (SpectraMax iD3 spectrophotometer, Molecular Devices). Day 1 acted as the baseline for the assessment of cell growth over time. The average of the six wells from day 1 for each line was used to normalize. The following formula was used to calculate growth for each day and cell line: $((\text{ending value} - \text{average starting value}) / \text{average starting value}) \times 100\%$. A line graph was generated showing the average growth for each day plus stan. dev. for each cell line.

Quantitative RealTime PCR (qRT-PCR)

Cells were harvested in Trizol (Invitrogen), and RNA was isolated according to the manufacturer's protocol. RNA concentration was quantitated on a Nanodrop Lite spectrophotometer (ThermoScientific). Synthesis of cDNA was done using high-capacity cDNA reverse transcription kit (Applied Biosystems). qRT-PCR was performed using PowerUp SYBR Green qPCR master mix (Applied Biosystems) on an Applied Biosystems-StepOnePlus. Fold change was calculated using the $2^{(-\Delta\Delta Ct)}$ method. [23]

Table 1: Primer sets used for qRT-PCR were as follows

Gene	Forward 5'	Reverse 5'
Slc20a1	TTCTTCCTGGTTCGTGCATT	CCAACCTGTGCAGGCATAGAA
Slc20a2	GACTCGCAGCTCCACGC	TTCCATATTTTTCCTCCCGA
Slc34a2	CTGAGGCACCTGTAACCAAGA	TGATCCCCGAGTCCTGAAGAG
OPN	AGGCTGATTCTGGAAGTTCTGAGG	ACTCCTCGCTTTCCATGTGTGAGG
CD44	GACAAGTTTTGGTGGCACG	ACGTGGAATACACCTGCAA
18S	CAGCCACCCGAGATTGAGCA	TAGTAGCGACGGGCGGTGTG

Migration/Invasion:

Cell migration assay was performed using Transwell (pore size, 8 μm ; Greiner Bio-One, Monroe, NC, USA) in a 24-well plate. Each A549 subpopulation was serum- and Pi-fasted for 24h before seeding 1×10^4 A549 cells in 200 μl of serum- and Pi-free medium in the upper chamber, and 500 μl of medium containing Pi (0.5, 1, or 5mM) and 2% FBS was placed in the lower chamber. The plate was incubated at 37°C in a humidified atmosphere containing 5% CO₂ for 24 h. At the end of the experiment, the cells that passed through the filters were stained with crystal violet (Fisher Scientific, Waltham, MA) solution and counted under a microscope (Nikon Eclipse TS100, Melville, NY). These experiments were performed in triplicate.

Colony formation:

A549 cells were seeded at 200 cells per well in 6-well plates and treated with various concentrations of Pi (0.5, 1, or 5mM) and in the presence or absence of Foscarnet (Pi inhibitor) (1mM) (Sigma). Cells were incubated at 37°C for 14 days without any disturbances. Following incubation, the medium was removed, and colonies were fixed with methanol and stained with

0.5% crystal violet (dissolved in 25% methanol). Colony counting was performed using Fiji/ImageJ software. [24] These experiments were performed three times in triplicates.

Statistics:

The data are expressed as the mean \pm SD. Statistical significance was determined using GraphPad Prism. Simple comparisons were made with unpaired Student's t-test and multiple comparisons were performed by repeated measures ANOVA.

Results:

FLIPPi FRET Free Phosphate Biosensor

A major obstacle to previous attempts to understand cellular Pi consumption related to tumorigenesis and metastasis has been an inability to track it due to its use in many cellular processes. Here we investigate the use a novel FRET-based sensor to try and overcome this hurdle. Fluorescence resonance energy transfer (FRET) microscopy is a tool that can be used to monitor intracellular interactions., by a process where energy is transferred between a donor molecule and an acceptor molecule which results in the emission of a fluorescent signal from the acceptor. In this case, the donor and acceptor molecules are two fluorophores that are fluorescent proteins. [25, 26] [25, 26] For this experiment, cyan fluorescent protein (CFP) (donor) and the yellow fluorescent protein (YFP) (acceptor) systems were used, a common fluorophore pair. [27] The fluorescence of these proteins can be measured at specific, expected wavelengths allowing FRET efficiency to be measured by monitoring changes in the fluorescent emissions of the donor and acceptor (Fig 1A). The gene transfected was the FLIPPi sensor or fluorescent indicator protein for Pi (Fig 1A). This FRET system had been demonstrated to show accurate monitoring of intracellular Pi levels within cells. As concentrations of Pi increase in the cytoplasm, Pi binds to the Pi-binding protein (PiBP) protein, eliminating the FRET signal (Fig

1A). Therefore, this system can tell us a relative estimate of Pi concentration in the cytoplasm of cells via the intensity of the FRET signal. [22]

A549 cells were used in this experiment, an NSCLC cell line, a common, effective model for lung cancer. [28] Stable transfection of the FRET sensor, FLIPPi, was accomplished using the Sleeping Beauty transposase system (Class II TE) to generate the stable parental line (Fig 1B). This method of transfection was used in this experiment to deliver the FRET system over more canonical methods, like the use of an adenovirus, retrovirus other related viruses because it is cleaner, more robust, and more efficient. [29-31] Unlike other gene-altering methods, transposons deliver the FRET system directly and efficiently, allowing the A549 cells to not be clonally selected. [29-31] Clonal selection would not be desirable in this experiment because we wanted to maintain the Pi heterogeneity of the different cell lines generated. Furthermore, the transposase system does not require homologous recombination, which is a DNA repair technique some systems utilize to properly transpose a target gene. That does not work with this system, because CFP and YFP have high homology. If homologous recombination was utilized, the construct could overexpress one protein. Therefore, that is not an issue in this case. [29-31]

The transposon vector containing the gene of interest, in this case, the FLIPPi cassette, and the transposase vector were transiently transfected using Lipofectamine (Invitrogen) in accordance with the manufacturer's protocol in a 5:1 ratio. After 48h the media was changed and cells expressing FLIPPi were selected for using puromycin (Fig 1C). Cells were then fluorescence-activated cell sorted (FACS) for YFP to eliminate any low or very high-expressing cells (Fig 1D, E). This creates a large parental population that has a more homogenous expression without impacting the heterogeneity of the phenotype. For the FACS sorting of the subpopulations, single cells were suspended in HBSS containing 1% FBS and 1mM EDTA (final

Pi 0.7mM) for FACS-FRET sorting using a FACS Aria II. To measure eCFP, FRET cells were excited with the 405 nm laser, and fluorescence was measured with a standard 450/40 filter for eCFP and a 529/24 filter for the FRET signal (Fig 1D). To measure YFP, cells were excited with the 488 nm laser, and emission was collected with a 529/24 filter. Cellular populations were sorted by high, low, or moderate FRET signal. Subpopulations were re-evaluated for FRET after 20 passages to ensure phenotypic stability.

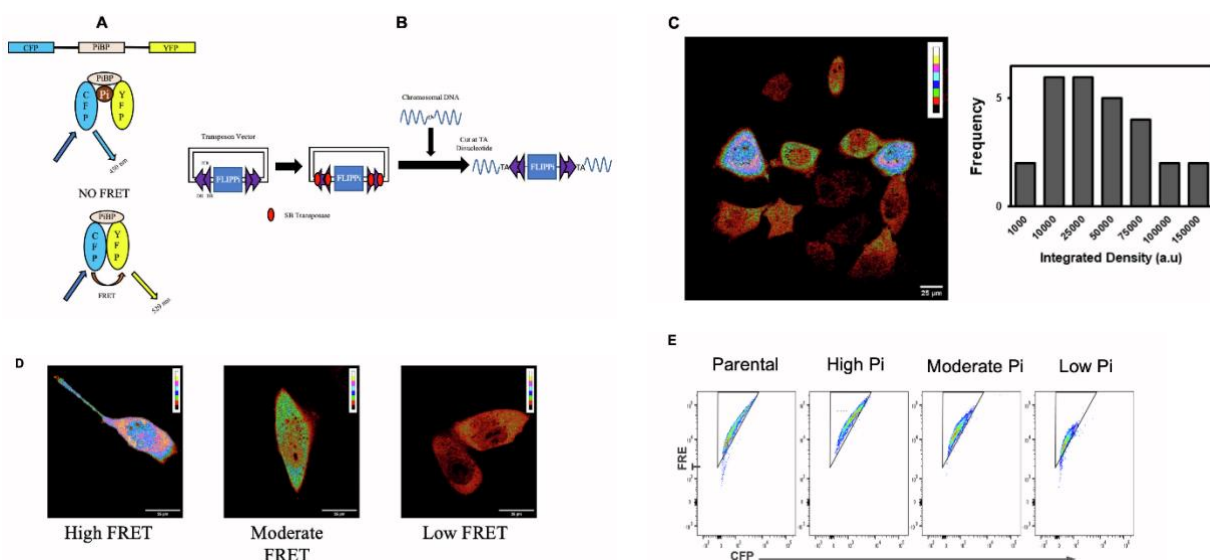


Figure 1. FLIPPi FRET Biosensor. (A) Model demonstrating the function of FLIPPi FRET sensor. FRET does not occur when Pi binds to the Pi-binding protein (PiBP), creating a distance between CFP and YFP. (B) Model demonstrating the function of the Sleeping Beauty Transposase system. SB transposase binds to DRs and cuts the chromosome at the TA dinucleotide. Then, a cut is made at the DRs and the FLIPPi cassette is transposed into the genome. (C) A549 cells expressing FLIPPi at 1mM Pi show heterogeneity in intracellular Pi levels. Representative image and distribution of Pi levels. n=25; magnification 40x. Scale bar = 25 μ m. (D) Representative images demonstrating intracellular in individual A549 cells in media containing 1mM Pi. Scale bar = 25 μ m. (E) FACS analysis of FRET in A549 parental and subpopulations.

Pi Consumption Levels Has Potential Influence on Growth and Proliferation.

To test whether Pi consumption levels influence the growth and proliferation of lung carcinoma epithelial cells, a growth time course assay was conducted. FRET-expressing cell lines, as well as parental cells, were plated at 500 cells/well in a normal growth medium. Cell viability was measured after 24 and 72hrs using an XTT assay. The experiment was performed twice. For both time courses, the low FRET subpopulation had a higher absolute cell viability value than both the moderate and high FRET subpopulations, on day 1 and day 3 (Fig 2A). Also, the low FRET subpopulation experienced a higher rate of change in cell viability from day 1 to day 3, in comparison to the high FRET group (Fig 2B). This tracks the predicted effect of Pi on the growth rate behavior of the cells. The overall results from this assay suggest that the high Pi consumer (low FRET) proliferates at a higher rate in standard growth medium and at basal levels of Pi (1 mM) than either moderate or low consumers.

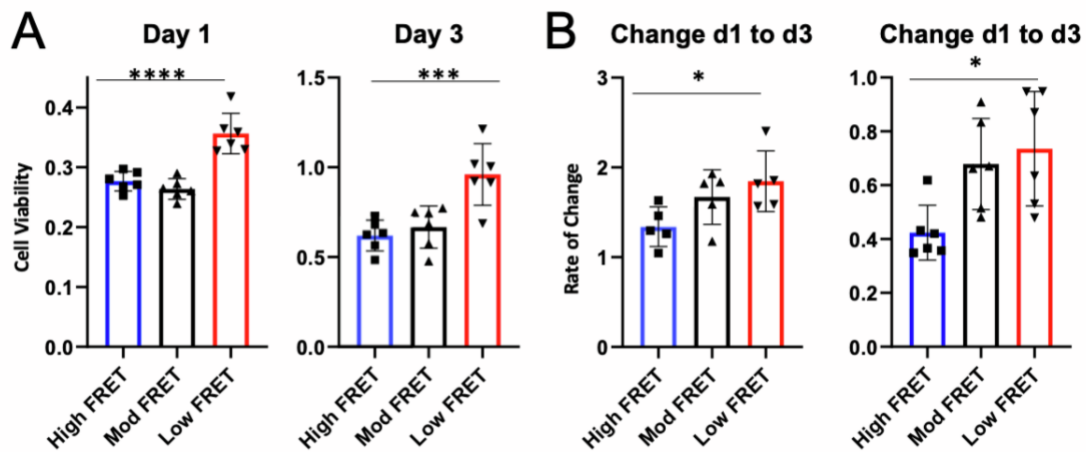


Figure 2. Growth and Proliferation rates are different between the Pi-consuming sub-populations. (A) High, Moderate, and Low FRET subpopulations were plated at 500 cells/per well, and XTT reagent was used to measure cell viability at 24 and 72 hrs (****P<0.005 & ***P<0.001 by One-way ANOVA); n=6.

(B) Each graph represents separate experiments. The rate of change was calculated as the increase from 24 to 72 hrs (*P<0.05 by One-way ANOVA); n=6.

High Pi consumers are more responsive to elevated phosphate

The ability of cells to grow as colonies under suboptimal growth conditions such as low density and minimal growth serum are considered representative of a “transformed” or pre-cancerous phenotype. To further test the cancer-related phenotype of our different Pi-consuming subpopulations, a clonogenic assay was performed. Cells were seeded at 200 cells/mL (low density) and allowed to grow for 14 days, in a low serum medium. After 14 days, the cells were fixed, stained, and imaged. Amongst all the subpopulations at baseline Pi levels (1mM), there was no significant difference in colony number (Fig. 3A, B). However, there was a significant difference in colony number between Pi treatments for the low FRET subpopulation in response to addition of Pi (Fig. 3A). This is suggestive that high Pi consumers have an increased capacity to respond to increases in extracellular Pi. To determine the role of Pi-transport in the process an inhibitor Foscarnet (phosphonoformic acid) was used. The use of the foscarnet treatment reduced most proliferation and growth from all the subpopulations and proved to have the biggest effect on the colonies (Fig. 3A, B). Taken together, the results suggest that basal Pi consumption does not influence the transformation of the A549 line of NSCLC cells, but that Pi transport is necessary for the process.

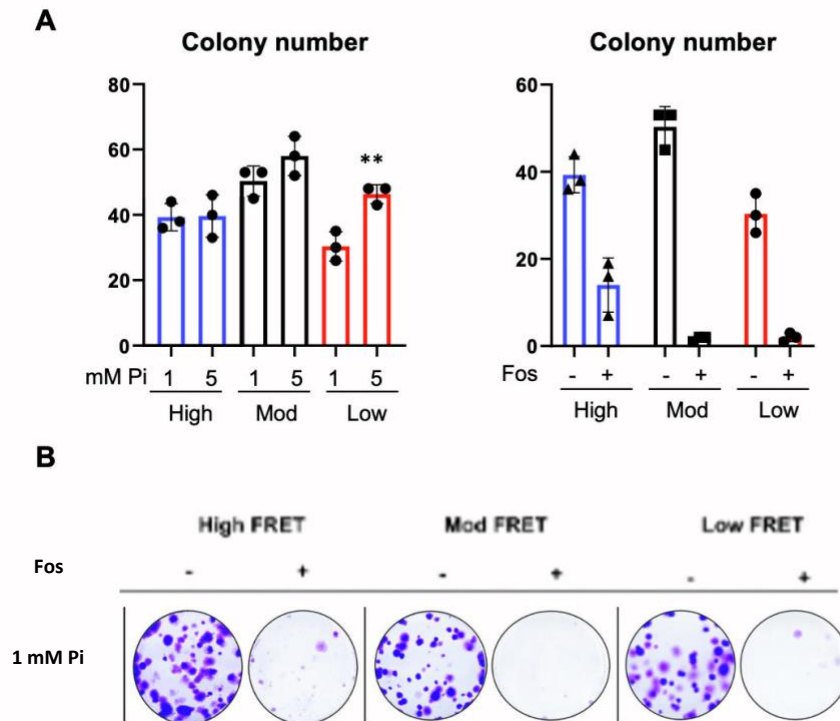


Figure 3. High Pi consumers do not form colonies at greater rates. The A549 subpopulations were seeded at 200 cells/mL and grown over 14 days at 37°C. Then they were fixed, stained, and imaged; n= 3(A) High, Moderate, and Low FRET subpopulations were treated with 1- and 5-mM Pi as indicated 24 hrs after seeding. Media was replaced as needed. Colony counting was performed using Fiji/ImageJ software (**P<0.01 by student's t-test). (B) Representative images of assay from (A) at 1 mM Pi and 1 mM Foscarnet (Fos).

High Pi Consumers Demonstrate Increased Migratory Phenotype

Cell migration is one important step in the development of metastases. Cells in culture can be assessed for migratory potential using an assay in which cells migrate through a membrane and are then counted. The transwell migration/invasion assay was completed to analyze and understand the effect that Pi has on different Pi consumers and their migratory phenotype. To do this, each subpopulation and treatment group were grown in media with 1 mM Pi. Cells were allowed to migrate for 24 hours, and those that migrated in the assay were stained

and counted (Fig. 4A). It was found that low FRET cells (high Pi consumers) showed an increased migratory phenotype in comparison to the high FRET subpopulations, at all Pi treatment levels (Fig. 4B). The low FRET sub population migration counts more than doubled between 1 mM and at 5 mM (Fig. 4B). These findings follow the hypothesis that high Pi consumer cells would show an increased and more aggressive migratory behavior, at optimal and excess Pi conditions. Foscarnet was also used in this assay to determine the requirement of Pi-transport on cell migration. Foscarnet decreased the migration of the high consumer subpopulation, most notably at the 5 mM Pi treatment (by more than two-fold) (Fig. 4C). This indicates that the inhibition of Pi consumption in high consumers decreases their migratory behavior, in excess Pi conditions. Overall, the transwell assay supports the hypothesis that high Pi consumer cell lines showed an increased migratory phenotype at the favorable and excess Pi conditions, and Pi transporter inhibition decreases cell migration.

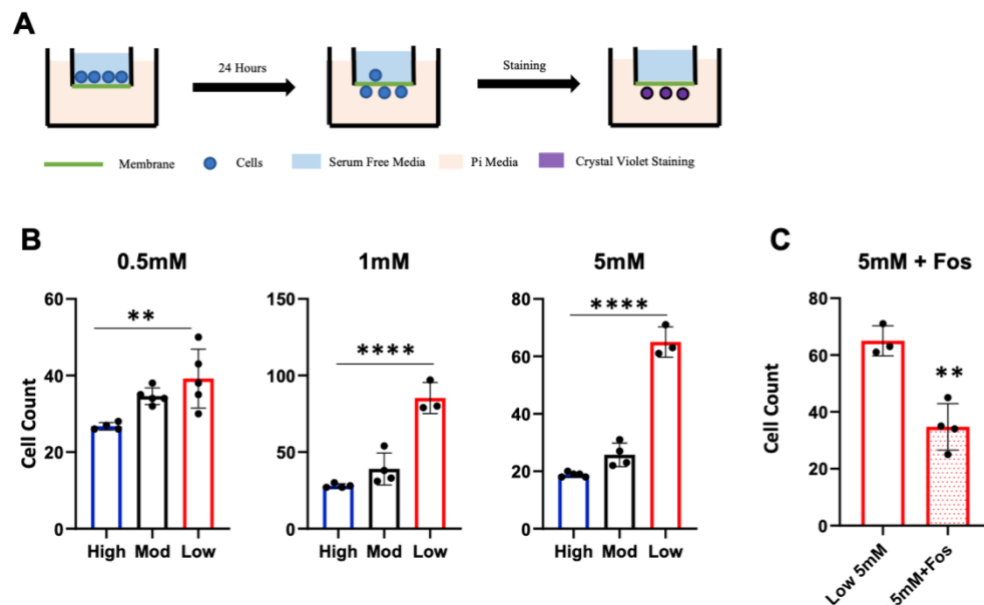


Figure 4. High Pi consumers demonstrate an increased migratory phenotype. (A) Model for Transwell Assay. 1×10^4 A549 cells were seeded in the upper chamber, and 500 μ L of Pi at 0.5, 1-, and 5-mM Pi and 2% FBS were placed in the lower chamber. Cells were allowed to migrate for 24 hours, and cells that

passed the membrane through were stained with crystal violet and counted under a microscope. (B) Samples were run at 0.5 mM Pi (**P<0.01), at 1 mM Pi (****P<0.0001), and at 5 mM Pi (****P<0.0001); all by One-way ANOVA; n=3,4 or 5. (C) Foscarnet was used at 1 mM in the same procedure as (A) (**P<0.01 by student's t-test); n=3, or 4.

Phosphate and Gene expression

Changes in gene expression represent a window on changes in cell behavior related to cancer progression. Quantitative Real-Time -PCR (qRT-PCR) analysis of genes related to Pi consumption, cancer metabolism, genesis, and metastasis was done to indicate how gene expression differs amongst the varying levels of Pi consumers. Pi cotransporter genes were analyzed to determine if Pi uptake was a factor in determining levels of Pi consumption among the subpopulations. The SLC34 and SLC20 family of transporters were analyzed. The SLC34a2 transporter demonstrated little to no expression in all the subpopulations at each Pi treatment, and the SLC20a2 showed no statistical difference in expression among between subpopulations for all treatments (Fig. 5A). However, the high FRET subpopulation demonstrated a significant difference in expression of SLC20a1 from the moderate and low FRET groups. The moderate FRET demonstrated a significant increase in expression compared to the low FRET group as well (Fig. 5A). Overall, the Pi transporters demonstrated some upregulation in low-Pi-consuming cells.

Osteopontin (OPN), is an important marker for gene metastasis and cancer progression and known to be Pi-responsive and therefore was a gene of interest. For the high FRET cells, a significant difference was not seen between the Pi treatment. For moderate FRET, a significant difference was seen between 1 mM and 3 mM Pi treatment, and for low FRET, 1 mM and 5 mM was (Fig. 5B). CD44, a metastasis-linked gene was also examined. For high FRET, the 1 mM

versus the 5 mM treatment demonstrated a significant difference in relative expression. For low FRET, the 1 mM versus 3 mM and 1 mM versus 5 mM Pi treatments demonstrated a significant difference (Fig. 5C). Overall, the high Pi-consuming cells demonstrated an upregulation of these metastasis-linked genes at excess Pi treatments.

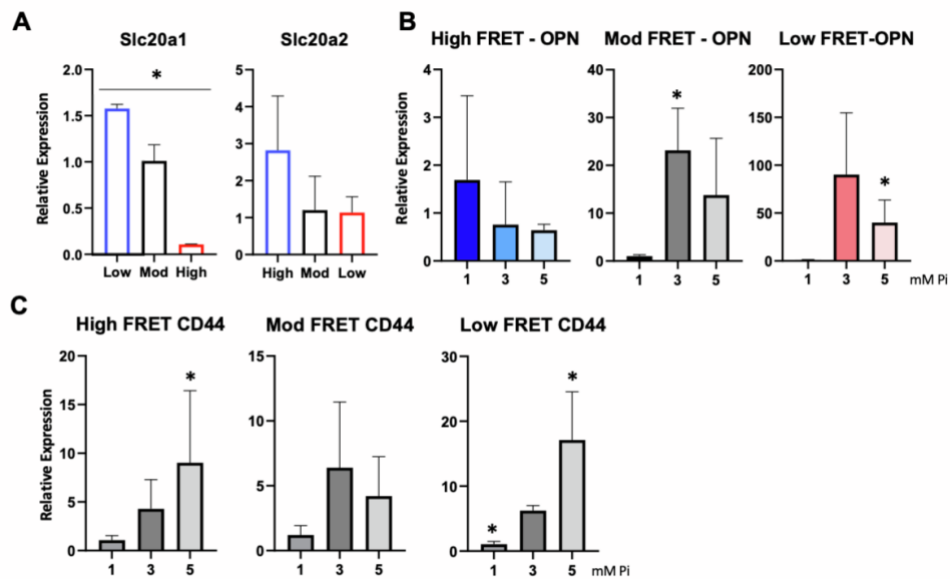


Figure 5. Changes in gene expression. qRT-PCR was performed to analyze genes. Fold change was calculated using the $2^{-\Delta\Delta Ct}$ method. These experiments were performed in triplicate. (A) RNA was harvested from proliferating FRET subpopulations and quantified using qRT-PCR; results expressed a relative expression to the Moderate FRET group samples run in triplicate ($P < 0.05$ by student's t-test) (B) High, Moderate, and Low FRET subpopulations were treated with increasing Pi concentrations as indicated for 72 hrs and cells harvested for RNA analysis by qRT-PCR; results relative to 1mM. Samples run in triplicate ($*P < 0.05$ by student's t-test) (C) Same procedures to (B) ($*P < 0.05$ by student's t-test).

Discussion:

Both proliferation and migration/motility are important markers for measuring cancer progression and aggression. For proliferation, a myriad of cell signaling pathways promotes an increase in metabolism and cell division, leading to an increase in cell growth. [32, 33] Pathways

that mediate this proliferation are negatively regulated, which over time will lead to carcinogenesis and the eventual formation of malignant tumors that migrate and invade distal tissue. [33, 34] This makes this process an important marker for the early stages of metastasis. Increased motility has been studied in relation to increased and decreased expression of many genes, metastasis-linked genes, like OPN. [35-37] Identifying targets related to this migratory phenotype, genetic or environmental factors, is important for identifying therapeutic interventions. Previous studies have already suggested the link between elevated Pi as an environmental factor that promotes this deadly phenotype. [21] This study demonstrates that subpopulations of heterozygous NSCLC cell lines exhibiting a phenotype for increased Pi consumption could be driving this behavior.

Results from the cell viability assay revealed that the Low FRET (high Pi consumer) subpopulation demonstrated an increase in both the absolute and percent change (proliferation) from day 1 to day 3. This demonstrates that high levels of Pi available in the cytoplasm have a positive effect on NSCLC cell proliferation potential. Previous studies in our lab and others have illustrated the role of Pi in cancer proliferation via increased mediation in non-cancerous cell types. [9, 14, 38] One explanation is suggested by the growth rate hypothesis, which states that cancer cells will have an increased demand for Pi due to its association with a myriad of energy metabolism factors (ex. ATP). [10] Furthermore, studies have shown that an excess of Pi has increased cell growth potential. [12, 39, 40] Possibly, high-Pi-consuming cells are a driving factor in this phenotype, even in tissues that are already experiencing a high rate of growth, like tumors. Whether the increased Pi consumption of this subpopulation is driving this increase or is a result of the cell demands of cell division is still to be determined. Understanding this cause-or-effect relationship will be important to further attempts to manipulate Pi availability for either

cancer prevention (excess Pi drives proliferation) or cancer treatment (cancer cells require excess Pi). These high Pi-consuming cells could not be driving just proliferation, but also cancer progression to a metastatic state.

OPN is a secreted phosphoprotein factor that has been shown in previous studies to respond strongly to elevated Pi availability [41-43] and is found to be positively associated in with progression to metastasis from varied cancers. [44, 45] OPN acts in a cytokine-like fashion, binding to transmembrane glycoproteins like CD44, which has been demonstrated to be overexpressed in many cancer models [46] However, the exact mechanistic role for modulation of OPN via Pi has yet to be elucidated. This study demonstrates that increased Pi availability leads to increased expression of OPN in high Pi-consuming cells. The transwell assay demonstrated that the high Pi consumer subpopulations were more migratory and motile at both optimal and excess Pi conditions. This finding could mean that high Pi-consuming cells are the driver of tumor progression and metastasis, with a link to OPN overexpression being a possible reason for this.

These findings suggested that cells with a high-Pi-consuming phenotype are showing more characteristics associated with cancer progression, which begged the question, “how are these high Pi-consuming cells acquiring more Pi?” One explanation is an increase in Pi transporters. Previous studies have found increased expression of Pi transporters (Slc43a2, Slc20a1,2) in cancer cells, including the lung, and this increase has been linked to tumor progression. [14, 19, 21, 47-49] Although gene expression studies did not detect the expression of the SLC34a2 transporter in any of our subpopulations, Slc20a1 and SLC20a2 were strongly identified. Upregulation of the Slc20a1 transporter was demonstrated in the low Pi consumers and downregulated in the high Pi consumers, opposite of what was expected if a change in

transporter abundance was to explain the increased consumption of the low FRET cells.

Although a western blot was not performed to confirm the gene expression data of Slc20a1 in the low Pi-consuming cells, the abundance of these transporters is generally thought to follow gene expression patterns. It is possible that a change in transporter import kinetics in response to changes in extracellular Pi levels could explain the difference in consumption. However, assays to measure these kinetics have not been currently developed. Overall, a change in Pi transporter expression did not explain why these high Pi-consuming cells are able to take advantage of Pi, however, the clonogenic assay still demonstrated how essential Pi transport was for the cells. Therefore, these Pi transporters still represent a novel target to manipulate cell behavior, and research on the topic is gaining interest.

The above results suggest that the high-Pi-consuming cells (Low FRET) have an increased proliferative profile and a more aggressive migratory profile. One explanation is that these cells have acquired a Pi “addiction”. If cancerous cells have acquired an “addiction” to Pi how might cells obtain additional Pi in vivo? One way is through diet. Serum Pi levels are proportional to Pi consumption. The American diet (2-4x recommended amount) is particularly high in Pi, found in colas, commercially prepared and processed foods, fast foods, and more. [5] High Pi environment throughout the tissues of the body could create conditions for cancer cells to operate optimally. The idea is supported by studies in mice. Mice models where mice were fed a diet high in Pi correlated to an increase in serum Pi, increasing tumor number, size, and proliferation. [14] Studies on humans are lacking, but one study showed a correlation between increased Pi intake and oncogene-driven tumorigenesis. [50] Changes to the diet could have positive impacts on health. [21]

An important consideration regarding the interpretation of the FRET data is that the changes in FRET could be attributed to an increase in metabolic activity, not necessarily an increase in actual Pi consumption. However, although indirect, the proliferation assay, in which the rate of change was calculated suggests that metabolism may not fully explain the result as the difference would be normalized between the time points. However, a future study that might directly answer this question is a Seahorse assay which is used to illustrate the rate of ATP production in each subpopulation, as a measure of metabolic activity. Furthermore, along with the seahorse assay mentioned earlier, an oxidative stress assay can be performed as another marker for cell metabolism. These assays, in conjunction with this FRET analysis, would help validate and provide clarity to the novel FRET sensor in this experiment.

Conclusions/Future directions

This experiment demonstrated that the novel FRET biosensor used can help detect intracellular Pi as a possible marker of Pi consumption. In the future, metabolic assays in conjunction with this sensor would help illustrate definitive Pi consumption differences between subpopulations. This experiment also demonstrated that high Pi consumers might be a driving factor in NSCLC progression regarding proliferation and metastasis.

NSCLC metastasis is interesting in the context of bone, as bone metastasis is close to 40% for lung cancer patients. [51] Approximately 85% of the Pi found in the body is stored in the bone, and as bone remodels, Pi is released. [52] Therefore, high Pi-consuming cancer cells could be seeking out this high Pi environment and taking advantage of this remodeling environment, relating back to this addiction cancer cells could be acquiring for Pi. [41, 43] Understanding this dynamic further is a compelling future direction.

Another interesting future direction is identifying a valuable therapeutic window in the control and treatment of NSCLC. The clonogenic assay demonstrated that the high Pi consumers were more heavily affected by Pi transporter inhibition than the other subpopulations. Foscaent was still too effective on the other subpopulations, but this is an interesting window of intervention. The role of Pi-induced OPN overexpression is still not fully known but targeting this overexpression in high-Pi consumers could help determine if OPN is a potential target.

References

1. Asai, N., et al., *Relapsed small cell lung cancer: treatment options and latest developments*. Ther Adv Med Oncol, 2014. **6**(2): p. 69-82.
2. Wang, X. and A.A. Adjei, *Lung cancer and metastasis: new opportunities and challenges*. Cancer Metastasis Rev, 2015. **34**(2): p. 169-71.
3. Weilbaecher, K.N., T.A. Guise, and L.K. McCauley, *Cancer to bone: a fatal attraction*. Nat Rev Cancer, 2011. **11**(6): p. 411-25.
4. Goretti Penido, M. and U.S. Alon, *Phosphate homeostasis and its role in bone health*. Pediatr Nephrol, 2012. **27**(11): p. 2039-2048.
5. Sapio, L. and S. Naviglio, *Inorganic phosphate in the development and treatment of cancer: A Janus Bifrons?* World J Clin Oncol, 2015. **6**(6): p. 198-201.
6. Brazy, P.C., et al., *Metabolic Requirement for Inorganic Phosphate by the Rabbit Proximal Tubule: EVIDENCE FOR A CRABTREE EFFECT*. The Journal of Clinical Investigation, 1982. **70**(1): p. 53-62.
7. Brazy, P.C., et al., *Interactions Between Phosphate Transport and Oxidative Metabolism in the Rabbit Proximal Tubule*, in *Regulation of Phosphate and Mineral Metabolism*, S.G. Massry, J.M. Letteri, and E. Ritz, Editors. 1982, Springer US: Boston, MA. p. 65-69.
8. Wilson, D.F., C.S. Owen, and A. Holian, *Control of mitochondrial respiration: A quantitative evaluation of the roles of cytochrome c and oxygen*. Archives of Biochemistry and Biophysics, 1977. **182**(2): p. 749-762.
9. Bobko, A.A., et al., *Interstitial Inorganic Phosphate as a Tumor Microenvironment Marker for Tumor Progression*. Sci Rep, 2017. **7**: p. 41233.
10. Elser, J.J., et al., *Biological stoichiometry in human cancer*. PLoS One, 2007. **2**(10): p. e1028.
11. Thomas, C.I., M.S. Bovington, and J.S. Krohmer, *Uptake of Radioactive Phosphorus in Experimental Tumors: I. Comparison of Radioactivity in Neoplastic and Normal Ocular Tissue**. Cancer Research, 1956. **16**(8): p. 796-803.
12. Camalier, C.E., et al., *Elevated phosphate activates N-ras and promotes cell transformation and skin tumorigenesis*. Cancer Prev Res (Phila), 2010. **3**(3): p. 359-70.
13. Holley, R.W., Kiernan, J.A., *Control of the Initiation of DNA Synthesis in 3T3 Cells: Low-Molecular-Weight Nutrients*. Proceedings of the National Academy of Sciences 1974. **71**: p. 2942-2945.

14. Jin, H., et al., *High dietary inorganic phosphate increases lung tumorigenesis and alters Akt signaling*. Am J Respir Crit Care Med, 2009. **179**(1): p. 59-68.
15. Slaga, T.J., et al., *The mouse skin carcinogenesis model*. The journal of investigative dermatology. Symposium proceedings, 1996. **1**(2): p. 151-156.
16. Lacerda-Abreu, M.A., et al., *Inorganic phosphate transporters in cancer: Functions, molecular mechanisms and possible clinical applications*. Biochim Biophys Acta Rev Cancer, 2018. **1870**(2): p. 291-298.
17. Biber, J., N. Hernando, and I. Forster, *Phosphate Transporters and Their Function*. Annual Review of Physiology, 2013. **75**(1): p. 535-550.
18. Segawa, H., et al., *The Role of Sodium-Dependent Phosphate Transporter in Phosphate Homeostasis*. Journal of Nutritional Science and Vitaminology, 2015. **61**(Supplement): p. S119-S121.
19. Vlasenkova, R., et al., *Characterization of SLC34A2 as a Potential Prognostic Marker of Oncological Diseases*. Biomolecules, 2021. **11**(12).
20. Virkki, L.V., et al., *Phosphate transporters: a tale of two solute carrier families*. Am J Physiol Renal Physiol, 2007. **293**(3): p. F643-54.
21. Arnst, J.L. and G.R. Beck, Jr., *Modulating phosphate consumption, a novel therapeutic approach for the control of cancer cell proliferation and tumorigenesis*. Biochem Pharmacol, 2021. **183**: p. 114305.
22. Gu, H., et al., *A novel analytical method for in vivo phosphate tracking*. FEBS Lett, 2006. **580**(25): p. 5885-93.
23. Livak, K.J. and T.D. Schmittgen, *Analysis of relative gene expression data using real-time quantitative PCR and the 2(-Delta Delta C(T)) Method*. Methods, 2001. **25**(4): p. 402-8.
24. Schindelin, J., et al., *Fiji: an open-source platform for biological-image analysis*. Nat Methods, 2012. **9**(7): p. 676-82.
25. Aoki, K., Y. Kamioka, and M. Matsuda, *Fluorescence resonance energy transfer imaging of cell signaling from in vitro to in vivo: basis of biosensor construction, live imaging, and image processing*. Dev Growth Differ, 2013. **55**(4): p. 515-22.
26. Sekar, R.B. and A. Periasamy, *Fluorescence resonance energy transfer (FRET) microscopy imaging of live cell protein localizations*. J Cell Biol, 2003. **160**(5): p. 629-33.
27. Dye, B.T., *Flow cytometric analysis of CFP-YFP FRET as a marker for in vivo protein-protein interaction*. Clinical and Applied Immunology Reviews, 2005. **5**(5): p. 307-324.
28. M.V. Croce, A.G.C., M.R. Price, A. Segal-Eiras, *Identification and characterization of different subpopulations in a human lung adenocarcinoma cell line (A549)*. Pathology & Oncology Research, 1999. **5**: p. 197-204.
29. Aronovich, E.L., R.S. McIvor, and P.B. Hackett, *The Sleeping Beauty transposon system: a non-viral vector for gene therapy*. Hum Mol Genet, 2011. **20**(R1): p. R14-20.
30. Kowarz, E., D. Löscher, and R. Marschalek, *Optimized Sleeping Beauty transposons rapidly generate stable transgenic cell lines*. Biotechnology Journal, 2015. **10**(4): p. 647-653.
31. Voigt, F., et al., *Sleeping Beauty transposase structure allows rational design of hyperactive variants for genetic engineering*. Nat Commun, 2016. **7**: p. 11126.
32. DeBerardinis, R.J., et al., *The biology of cancer: metabolic reprogramming fuels cell growth and proliferation*. Cell Metab, 2008. **7**(1): p. 11-20.

33. Feitelson, M.A., et al., *Sustained proliferation in cancer: Mechanisms and novel therapeutic targets*. *Semin Cancer Biol*, 2015. **35 Suppl**(Suppl): p. S25-S54.
34. Gupta, G.P. and J. Massague, *Cancer metastasis: building a framework*. *Cell*, 2006. **127**(4): p. 679-95.
35. Loh, C.Y., et al., *The E-Cadherin and N-Cadherin Switch in Epithelial-to-Mesenchymal Transition: Signaling, Therapeutic Implications, and Challenges*. *Cells*, 2019. **8**(10).
36. Kang, Y. and J. Massague, *Epithelial-mesenchymal transitions: twist in development and metastasis*. *Cell*, 2004. **118**(3): p. 277-9.
37. Rangaswami, H., A. Bulbule, and G.C. Kundu, *Osteopontin: role in cell signaling and cancer progression*. *Trends Cell Biol*, 2006. **16**(2): p. 79-87.
38. Lin, Y., et al., *Inorganic phosphate induces cancer cell mediated angiogenesis dependent on forkhead box protein C2 (FOXC2) regulated osteopontin expression*. *Mol Carcinog*, 2015. **54**(9): p. 926-34.
39. Conrads, K.A., et al., *A combined proteome and microarray investigation of inorganic phosphate-induced pre-osteoblast cells*. *Mol Cell Proteomics*, 2005. **4**(9): p. 1284-96.
40. Chang, S.H., et al., *Elevated inorganic phosphate stimulates Akt-ERK1/2-Mnk1 signaling in human lung cells*. *Am J Respir Cell Mol Biol*, 2006. **35**(5): p. 528-39.
41. Beck, G.R., Jr., *Inorganic phosphate as a signaling molecule in osteoblast differentiation*. *J Cell Biochem*, 2003. **90**(2): p. 234-43.
42. Foster, B.L., et al., *Regulation of cementoblast gene expression by inorganic phosphate in vitro*. *Calcif Tissue Int*, 2006. **78**(2): p. 103-12.
43. Beck, G.R., Jr., B. Zerler, and E. Moran, *Phosphate is a specific signal for induction of osteopontin gene expression*. *Proc Natl Acad Sci U S A*, 2000. **97**(15): p. 8352-7.
44. Wai, P.Y. and P.C. Kuo, *The role of Osteopontin in tumor metastasis*. *J Surg Res*, 2004. **121**(2): p. 228-41.
45. Oates AJ, B.R., Rudland PS, *The role of osteopontin in tumorigenesis and metastasis*. 1997. **17**(1): p. 1-15.
46. Naor, D.S., R.; Ish-Shalom, D.,; *CD44: Structure, Function and Association with the Malignant Process*. *Adv. Cancer Res.*, 1997. **71**: p. 241-319.
47. Jin, H., et al., *High dietary inorganic phosphate affects lung through altering protein translation, cell cycle, and angiogenesis in developing mice*. *Toxicol Sci*, 2007. **100**(1): p. 215-23.
48. Kimata, M., et al., *Signaling of extracellular inorganic phosphate up-regulates cyclin D1 expression in proliferating chondrocytes via the Na⁺/Pi cotransporter Pit-1 and Raf/MEK/ERK pathway*. *Bone*, 2010. **47**(5): p. 938-47.
49. Li, X., H.Y. Yang, and C.M. Giachelli, *Role of the sodium-dependent phosphate cotransporter, Pit-1, in vascular smooth muscle cell calcification*. *Circ Res*, 2006. **98**(7): p. 905-12.
50. Wilson, K.M., et al., *Calcium and phosphorus intake and prostate cancer risk: a 24-y follow-up study*. *Am J Clin Nutr*, 2015. **101**(1): p. 173-83.
51. Scagliotti, G.V., et al., *Overall survival improvement in patients with lung cancer and bone metastases treated with denosumab versus zoledronic acid: subgroup analysis from a randomized phase 3 study*. *J Thorac Oncol*, 2012. **7**(12): p. 1823-1829.
52. Khoshniat, S., et al., *The emergence of phosphate as a specific signaling molecule in bone and other cell types in mammals*. *Cell Mol Life Sci*, 2011. **68**(2): p. 205-18.